6 | Generalization:

The MPS in Eq. (9.10) treats the first and last spin differently (their matrices are actually vectors). This seems fine if we consider a 1D system with *open* boundary conditions. However, the above construction is generic (it does not know about boundary conditions or the Hamiltonian). For systems with *periodic* boundaries these special matrices seem out of place …

i | Motivation: ◁ Bosonic SSH chain with PBC

Ground state (8.29):

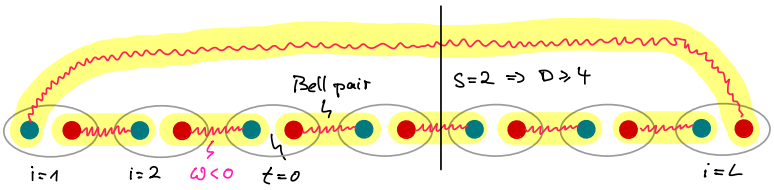

$\rightarrow D \geq 2^{S_{\max}} = 2^2 = 4$

This is the bond dimension required for an *exact* MPS representation of this ground state.

Note that one bit of entanglement entropy (and therefore one factor of 2 for the bond dimension) is due to the "long range" Bell pair that connect the two spins on the "boundary" (which is now an artifact of the MPS expansion that ignores the periodicity of the system).

→ More natural picture (that respects the PBC):

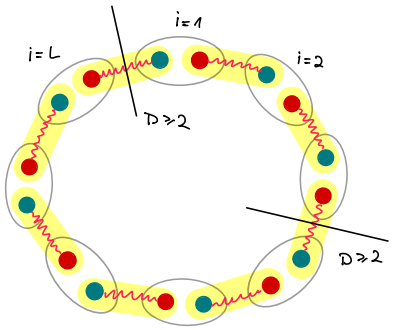

If the bond dimension reflects the entanglement "crossing a bond," this structure should be more efficient and require only $D = 2$ (as compared to $D = 4$ above).

→ We need a "Periodic" matrix product …

ii | ◁ Trace of matrix product:

$$|\Psi\rangle = \sum_{\boldsymbol{i}} \mathrm{Tr}\left[M^{[1]}_{i_1} \cdot M^{[2]}_{i_2} \cdot \ldots \cdot M^{[L-1]}_{i_{L-1}} \cdot M^{[L]}_{i_L}\right] |i_1 i_2 \ldots i_{L-1} i_L\rangle \tag{9.21}$$

"Taking the trace" is equivalent to *contracting* the two virtual indices of the matrix product!

→ Pictorial representation:

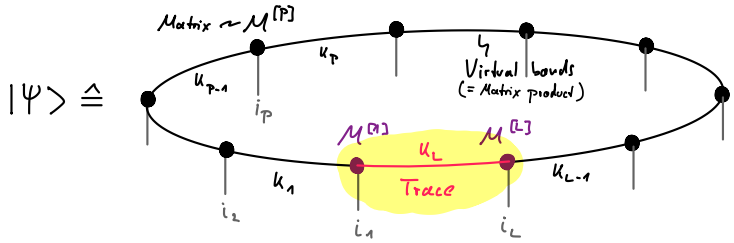

- The form (9.21) generalizes (9.10) in that the first reduces to the latter if $M_{i_1}^{[1]}$ and $M_{i_L}^{[L]}$ are row and columns vectors, respectively.
- Due to the cyclicity of the trace, the expression in Eq. (9.21) no longer picks out two sites as special (which has no physical significance for PBC). All matrices $M_{i_p}^{[p]}$ are now treated on the same footing for $p = 1, \ldots, L$ and can have arbitrary bond dimensions (matching their left and right neighbors).
- In general, periodic MPS of the form (9.21) do not have a canonical form (9.8) where the virtual indices at each bond label orthonormal left- and right Schmidt vectors because one cannot split the system into two parts by cutting a single bond.

iii | Example:

We consider again the two fixpoint wave functions of the two phases of the bosonic SSH chain. As shown in Section 8.3, both satisfy $S_{\max} = \text{const}$ (independent of L), thus we should expect efficient MPS representations:

- Phase A:

  It is convenient to group the two spins *on each unit cell* to one degree of freedom:

$$|A\rangle \overset{8.29}{=} \bigotimes_{n=1}^{L} \Big(\overbrace{|0\rangle_{2n}|1\rangle_{2n+1}}^{\text{Spins on } \textit{adjacent} \text{ unit cells!}} + |1\rangle_{2n}|0\rangle_{2n+1} \Big) \tag{9.22a}$$

$$\overset{!}{=} \sum_{\boldsymbol{i}} \operatorname{Tr}\left[A_{i_1 i_2}^{[1]} A_{i_3 i_4}^{[2]} \ldots A_{i_{2L-1} i_{2L}}^{[L]} \right] |i_1 i_2, i_3 i_4, \ldots, i_{2L-1} i_{2L}\rangle \tag{9.22b}$$

  ¡! Here we use $n = 1, \ldots, L$ for the spin indices to distinguish them from the spin states $i \in \{0, 1\}$ (which is the convention used throughout this section).

  → $d = 2 \cdot 2 = 4$

  ∘→ We only need 4 matrices to specify the complete state:

$$\left(A_{ii'}^{[p]}\right)_{kk'} = \delta_{ik} \sigma^x_{i'k'} \qquad \text{Check this!} \tag{9.23}$$

  Explicitly:

$$A_{00}^{[p]} = \begin{bmatrix} 0 & 1 \\ 0 & 0 \end{bmatrix} \quad A_{01}^{[p]} = \begin{bmatrix} 1 & 0 \\ 0 & 0 \end{bmatrix} \quad A_{10}^{[p]} = \begin{bmatrix} 0 & 0 \\ 0 & 1 \end{bmatrix} \quad A_{11}^{[p]} = \begin{bmatrix} 0 & 0 \\ 1 & 0 \end{bmatrix} \tag{9.24}$$

  with …

  - $d = 4$ states $ii' \in \{00, 01, 10, 11\}$

- virtual indices $k, k' \in \{0, 1\}$ with bond dimension $D = 2$

  The bond dimension $D = 2$ is required due to the Bell pair (entanglement) shared between adjacent sites.

- site index $p = 1, \ldots, L$

¡! The L matrices are the same for all sites p since the state is translation invariant.

- Phase B:

$$|B\rangle \overset{8.31}{=} \bigotimes_{n=1}^{L} \overbrace{(|0\rangle_{2n-1}|1\rangle_{2n}}^{\text{Spins on } \textit{same} \text{ unit cell!}} + |1\rangle_{2n-1}|0\rangle_{2n}) \tag{9.25a}$$

$$\overset{!}{=} \sum_{\boldsymbol{i}} \mathrm{Tr}\left[B^{[1]}_{i_1 i_2} B^{[2]}_{i_3 i_4} \ldots B^{[L]}_{i_{2L-1} i_{2L}}\right] |i_1 i_2, i_3 i_4, \ldots, i_{2L-1} i_{2L}\rangle \tag{9.25b}$$

$\overset{\circ}{\rightarrow}$ Again, we need 4 matrices to specify the complete state:

$$\left(B^{[p]}_{ii'}\right)_{kk'} = \sigma^x_{ii'} \qquad \text{Check this!} \tag{9.26}$$

Explicitly:

$$B^{[p]}_{00} = [0] \quad B^{[p]}_{01} = [1] \quad B^{[p]}_{10} = [1] \quad B^{[p]}_{11} = [0] \tag{9.27}$$

with …

- $d = 4$ states $ii' \in \{00, 01, 10, 11\}$
- virtual indices $k, k' \in \{0\}$ with bond dimension $D = 1$

  The bond dimension $D = 1$ is sufficient because there is no entanglement shared between adjacent sites. Consequently, k and k' are dummy indices.

  Hence the trace in Eq. (9.25b) is not necessary.

- site index $p = 1, \ldots, L$

Again, the L matrices are the same for all sites p since the state is translation invariant.

¡! Note that both states represent the optimal situation for MPS encodings: First, they can be *exactly* written in MPS form for $D \ll d^L$, and second, the bond dimension D is constant and independent of the system size L. This situation is *not* typical and a special feature of the fixpoint wave functions.

iv | These examples foster two insights:

- Boundary conditions:

  Adapting the topology of the bond contractions to the physical situation allows for more efficient MPS encodings (= smaller bond dimensions):

$$\text{Open boundary conditions} \quad \rightarrow \quad \text{Eq. (9.10) (no trace)} \tag{9.28a}$$

$$\text{Periodic boundary conditions} \quad \rightarrow \quad \text{Eq. (9.21) (trace)} \tag{9.28b}$$

  - Remember that both forms are universal as they can encode arbitrary quantum states. This distinction is only about *optimizing* (= lowering) the bond dimensions (= sizes of matrices).

- For technical reasons, one often uses open boundary MPS states in numerical algorithms like → *DMRG* (Section 9.2) *even for periodic systems*. The reason is that computing expectation values (Section 9.2) scales much worse (in D) for periodic MPS, so that the additional bond dimension one pays by not adapting the MPS topology to the physical situation is often worth the trade-off.

- Translation invariance:

  If the system Hamiltonian is *translation invariant* and does not break this symmetry spontaneously (which is the situation we are interested in), the ground state is also translation invariant. In this case, the MPS description becomes significantly more efficient since only a single set of d matrices is needed to encode the many-body state for arbitrary L:

$$|\Psi\rangle = \sum_{\boldsymbol{i}} \mathrm{Tr}\left[M_{i_1} M_{i_2} \dots M_{i_L}\right] |i_1 i_2 \dots i_L\rangle \tag{9.29}$$

  → ⁂ *Translation invariant MPS*

7 | Area- vs. volume laws in condensed matter systems:

So far, we were only concerned with many-body *states*. Hamiltonians were not important. So how can MPS representations help us to study quantum many-body phases described by a family of Hamiltonians?

i | Plot $S[A_l]$ as a function of subsystem size $l = 0, \dots, L$

→ Entanglement profile:

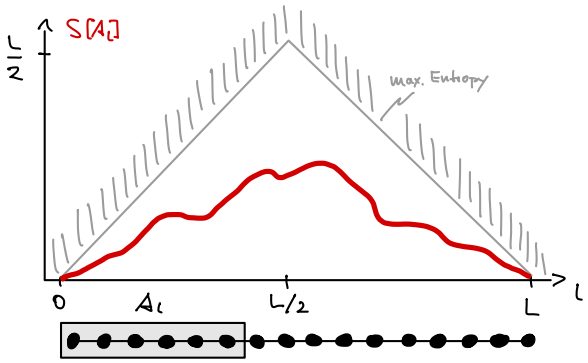

- It must be $S[A_0] = 0$ and $S[A_L] = 0$ since both A_l and the complement $\bar{A}_l$ must be non-empty sets for non-vanishing entanglement.
- Since $S[A_l] \overset{8.24}{\leq} \log_2 R_l \leq \log_2 \min\{d^l, d^{L-l}\} = \min\{l, L-l\} \cdot \log_2 d$, the entanglement profile of a state is always contained in the gray triangular region (shown for $d = 2$).

ii | ◁ Random states picked from the full Hilbert space $\mathcal{H}$:

Page [217–220] $\overset{*}{\rightarrow}$

$$\underbrace{\langle S[A_l] \rangle \sim l}_{\text{⁂ Volume law}} \quad \Rightarrow \quad \langle S_{\max} \rangle \sim L \tag{9.30}$$

Here $\langle \bullet \rangle$ denotes the average over all states in the Hilbert space.

In general, we say that $S[A]$ obeys a *volume law* if the entanglement of the subsystem A scales with its *volume* (= number of elementary subsystems). In 1D, the volume of an interval A_l is simply its length l.

→

Random states are volume-law entangled. ☹

- This is bad new because Eq. (9.13) forbids efficient MPS representations for such states.

  This is also true if one is satisfied with MPS *approximations*: One can show that a linearly growing entanglement entropy necessitates exponentially growing bond dimensions to achieve constant errors [215].

- Picking states "random" from the Hilbert space requires the definition of a probability distribution on $\mathcal{H}$ (mathematically: a ↑ *probability measure*). To this end, one chooses the ↑ *Haar measure* since it is the most natural one (it is the unique measure invariant under unitary transformations). This choice makes the average $\langle \bullet \rangle$ well defined.

- *Fun fact:* The exact result for $\langle S[A_l] \rangle$ is known as the ↑ *Page curve* (for small subsystems it is slightly less than the maximal allowed entropy). It plays a crucial role for solving the ↑ *black hole information paradox* [221, 222] put forward by Stephen Hawking [223]. (Don Page was a PhD student of Stephen Hawking.)

iii | Luckily we are not interested in *random* states …

◁ Ground states of gapped Hamiltonians in 1D

Remember the ground states of the ← *bosonic SSH chain*:

$$\text{Phase A:} \quad \text{Eq. (8.29)} \quad \Rightarrow \quad S[A_l] = 2 = \text{const} \tag{9.31a}$$

$$\text{Phase B:} \quad \text{Eq. (8.31)} \quad \Rightarrow \quad S[A_l] = 0 = \text{const} \tag{9.31b}$$

→ This suggests that in both gapped phases the entanglement is bounded by a constant:

$$\underbrace{S[A_l] \leq \text{const}}_{\text{⁂ Area law (in 1D)}} \quad \Rightarrow \quad S_{\max} \leq \text{const} \tag{9.32}$$

¡! In general, we say that $S[A]$ obeys an *area law* if the entanglement of the subsystem A scales with its *surface area*. In 1D, the surface area of an interval A_l is composed of two points and therefore constant in size.

It turns out that this scaling is no peculiarity of the bosonic SSH chain:

Hastings [28] $\xrightarrow{*}$

Ground states of gapped Hamiltonians in 1D are *area-law* entangled. ☺

→ Such ground states can be efficiently approximated by MPS!

This statement is made rigorous → *below*.

- The combinations of the results by Page and Hastings demonstrates that the ground states of gapped Hamiltonians are *not* typical states in the many-body Hilbert space: these states are rare and have special structure! This provides leverage for their description and classification …

- That (and how) ground states of gapped 1D systems can be approximated by MPS is a consequence of the following arguments:

  First, to quantify entanglement, we must replace the von Neumann entropy $S = -\operatorname{Tr}[\rho \log_2 \rho]$ of the reduced density matrix ρ in Eq. (8.18) by ⁂ *Rényi entropies*

  $$S^\alpha(\rho) := \frac{\log_2 \operatorname{Tr}[\rho^\alpha]}{1-\alpha} \tag{9.33}$$

  where $\alpha \geq 0$ and one recovers the von Neumann entropy in the limit $\alpha \to 1$.

  Next, HASTINGS not only showed that gapped 1D systems satisfy area laws in the von Neumann entropy, but also in Rényi entropies for $0 < \alpha < 1$ large enough [28]:

  $$S^\alpha[A_p] \overset{*}{\leq} S_{\max}\,, \tag{9.34}$$

  independent of $p = 1, \ldots, L-1$ and L.

  One can then prove an upper bound on the errors in Eq. (9.17) using the Rényi entropy [216]:

  $$\log_2 \epsilon_p(D) \overset{*}{\leq} \frac{1-\alpha}{\alpha}\left[S^\alpha(A_p) - \log_2\left(\frac{D}{1-\alpha}\right)\right]. \tag{9.35}$$

  With this and the area law, one finds the error on the MPS approximation

  $$\| |\Psi\rangle - |\Psi_D\rangle \|^2 \overset{9.16}{\leq} \text{const} \cdot L \cdot \frac{2^{\text{const}\cdot S_{\max}}}{D^{\text{const}}} \tag{9.36}$$

  where the constants depend on α.

- For more details on the efficient approximation of gapped ground states of one-dimensional quantum systems by matrix product states see ↑ Refs. [215, 216, 224, 225].
- Hastings' bound on the entanglement entropy was later improved by ARAD *et al.* [226].
- It is believed that the ground states of gapped Hamiltonians in *two* dimensions also obey an area law (at least all known examples have this property). To my knowledge, this has not yet been proven rigorously. Note that it has been proven (in any dimension) that (connected) *two-point correlations* decay exponentially in gapped systems [27]. Unfortunately, exponentially decaying correlations do not imply an area law without further qualifications [225] (although in many practical situations these two features go hand in hand). In any case, matrix product states must be generalized to → *tensor network states* (Section 9.3) to adapt the contraction geometry to higher spatial dimensions.
- The fact that ground states of gapped 1D systems can be efficiently approximated by matrix product states allows for a well-behaved numerical algorithm to find and characterize ground states of such systems. For historical reasons, this technique is known as → *density matrix renormalization group (DMRG)* (we briefly sketch this approach in Section 9.2). By now there are multiple mature software packages that can be used to apply this method off-the-shelf (➔ Problemset 11 and Refs. [227, 228]). This algorithm (and its various modifications) has expanded our understanding of strongly correlated quantum systems in one dimension significantly over recent years.

Summary:

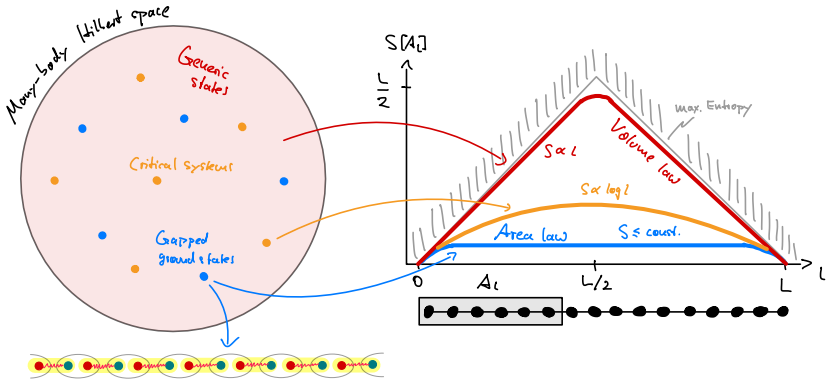

Here we also added the special case of *critical systems* (orange), i.e., the ground states of Hamiltonians tuned to a second order phase transition. These typically satisfy $S[A_l] \sim \log_2 l$ and therefore $S_{\max} \sim \log_2 L$ which still allows for efficient MPS approximations.

8 | Conclusion:

> Ground states of *gapped phases in 1D* can be approximated (with bounded error) by *matrix product states* with (at most) polynomially growing bond dimension.

We will use this fact to classify arbitrary (interacting!) topological phases in 1D.

9.2. ‡ Density matrix renormalization group (DMRG)

At this point, matrix product states are simply an alternative way to encode generic quantum states. Since they allow for efficient compression of states with low entanglement, and controlled approximations by dropping small Schmidt coefficients, they are are a versatile tool to study interacting quantum systems *numerically*:

9 | Expectation values of local observables:

In order to extract physically relevant quantities, one needs an efficient method to compute expectation values of observables from a given MPS:

i | ◁ Local observable

$$\boldsymbol{O} = \mathbb{1}_1 \otimes \ldots \otimes \mathbb{1}_{p-1} \otimes O \otimes \mathbb{1}_{p+2} \ldots \mathbb{1}_L \tag{9.37}$$

acting on two adjacent sites p and $p+1$:

$$\langle \Psi | \boldsymbol{O} | \Psi \rangle = \sum_{\boldsymbol{i},\boldsymbol{i}'} \bar{\Psi}_{\boldsymbol{i}} \Psi_{\boldsymbol{i}'} \delta_{i_1 i_1'} \ldots \underbrace{\langle i_p, i_{p+1} | O | i_p', i_{p+1}' \rangle}_{\equiv O^{i_p', i_{p+1}'}_{i_p, i_{p+1}}} \ldots \delta_{i_L i_L'} \tag{9.38}$$

ii | MPS picture: $\Psi_{\boldsymbol{i}} = A^{[1]}_{i_1} \cdot \ldots \cdot A^{[L]}_{i_L}$ (open boundaries!) →

$$\langle \Psi | \boldsymbol{O} | \Psi \rangle =$$

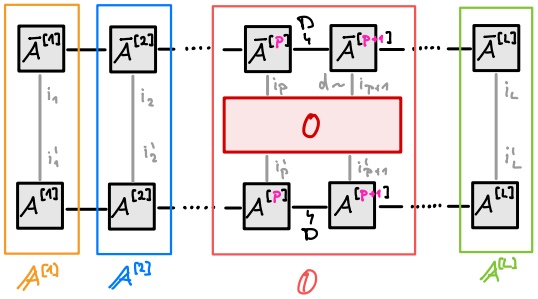

(9.39a)

$$= \underbrace{\overbrace{\mathbb{A}^{[1]}}^{D^2\text{-vector}} \cdot \overbrace{\mathbb{A}^{[2]} \cdot \ldots \cdot \mathbb{A}^{[p-1]} \cdot \mathbb{O} \cdot \mathbb{A}^{[p+2]} \cdot \ldots}^{D^2 \times D^2\text{-matrices}} \cdot \overbrace{\mathbb{A}^{[L]}}^{D^2\text{-vector}}}_{\text{Iterative product of } D^2\text{-vectors with } D^2 \times D^2\text{-matrices}} \tag{9.39b}$$

→ $\mathcal{O}(D^4)$ operations per matrix-vector product

→ $\mathcal{O}(LD^4)$ operations to evaluate expectation value

If $D = \text{const}$ (e.g., for gapped ground states), this scales linearly with the system size L!

iii | ◁ Local Hamiltonian $H = \sum_p \boldsymbol{O}_p$

→ Energy expectation value:

(It is often convenient to compute with MPS that are not normalized.)

$$E_\Psi := \frac{\langle \Psi | H | \Psi \rangle}{\langle \Psi | \Psi \rangle} = \underbrace{\sum_{p=1}^{L} \overbrace{\langle \Psi | \boldsymbol{O}_p | \Psi \rangle}^{\mathcal{O}(LD^4)\text{ ops.}}}_{\mathcal{O}(L^2 D^4)\text{ ops.}} \times \underbrace{\langle \Psi | \mathbb{1} | \Psi \rangle^{-1}}_{\mathcal{O}(LD^4)\text{ ops.}} \tag{9.40}$$

→ E_Ψ can be evaluated with $\mathcal{O}(L^2 D^4)$ operations

Again, for $D = \text{const}$ this is polynomial in the system size L!

- Using clever summation techniques, this scaling can be improved to $\mathcal{O}(LD^3)$ [214, 228].

- Using similar tricks, one can evaluate correlation functions of the form $\langle\Psi|\boldsymbol{O}_p\boldsymbol{O}_q|\Psi\rangle$ also with $\mathcal{O}(LD^3)$ operations [214, 228]. You apply this on ➔ Problemset 10.
- For *periodic* boundary conditions, the scaling of evaluating inner products and expectation values scales worse in the bond dimension due to the trace, namely as $\mathcal{O}(LD^5)$ [214, 228].

10 | Variational ground states:

To study the phase diagram of a given parametric family of Hamiltonians, we need to compute their ground states. The greatest strength of the MPS representation is that it allows for an efficient (= polynomial) algorithm to find (approximate) ground states even of strongly interacting systems:

i | ◁ 1D Hamiltonian $H = \sum_p \boldsymbol{O}_p$ →

$$\forall|\Psi\rangle \in \mathcal{H}: \quad \frac{\langle\Psi|H|\Psi\rangle}{\langle\Psi|\Psi\rangle} = E_\Psi \geq E_0 = \langle\text{Ground state energy}\rangle \tag{9.41}$$

ii | Idea:

- Parametrize $|\Psi\rangle$ as MPS: $|\Psi\rangle = |\{M_i^{[p]}\}\rangle$
- Vary matrices $\{M_i^{[p]}\}$ to minimize E_Ψ

If the ground state can be approximated by an MPS with small bond dimension (which it can for 1D gapped systems, ← *above*), this should automatically produce a good approximation of the ground state once we reach the minimum E_0 of E_Ψ.

We can check how close we are to an eigenstate (e.g., the ground state) by computing the variance of the Hamiltonian $\sigma_H^2(\Psi) = \langle\Psi|H^2|\Psi\rangle - \langle\Psi|H|\Psi\rangle^2$ (which can be done efficiently because $\langle\Psi|H^2|\Psi\rangle$ can be evaluated efficiently by the method sketched ← *above*). For an eigenstate $|\Psi\rangle$ of H it is $\sigma_H^2(\Psi) = 0$. If we minimize E_Ψ, wait until it saturates, and then check that $\sigma_H^2(\Psi) \approx 0$, we can be quite confident that we are close to the ground state. (We cannot be *sure* because we cannot exclude the possibility that we got "stuck" and converged to an excited state instead. However, in practice, this methods often works very well.)

iii | The minimization procedure works as follows:

a | Initialize MPS $|\Psi\rangle = |\{M_i^{[p]}\}\rangle$ e.g. with random matrices

Choosing a good initial state can influence the convergence of the algorithm.

b | Fix matrices on all sites except for one (p): $|\Psi\rangle \equiv |M^{[p]}\rangle$

Here $M^{[p]}$ stands for all entries of the matrices $M_i^{[p]}$ for $i = 1, \ldots, d$.

→ We want to minimize the function

$$E[M^{[p]}] := \frac{\langle M^{[p]}|H|M^{[p]}\rangle}{\langle M^{[p]}|M^{[p]}\rangle} \equiv \frac{\boldsymbol{M}^\dagger \mathbb{H}_p \boldsymbol{M}}{\boldsymbol{M}^\dagger \mathbb{N}_p \boldsymbol{M}} =: E[\boldsymbol{M}] \tag{9.42}$$

Here we used that $|M^{[p]}\rangle$ is a *linear* function of $M^{[p]}$.

with

- $\boldsymbol{M}$: vectorized dD^2 entries of $M^{[p]} = \{M_1^{[p]}, \ldots, M_d^{[p]}\}$

- $\mathbb{H}_p$: effective Hamiltonian (can be efficiently evaluated)

  $\mathbb{H}_p$ is the tensor contraction of $\langle\Psi|H|\Psi\rangle$ without matrices $M^{[p]}$.
- $\mathbb{N}_p$: normalization matrix (can be efficiently evaluated)

  $\mathbb{N}_p$ is the tensor contraction of $\langle\Psi|\Psi\rangle$ without matrices $M^{[p]}$.

c | Minimize Eq. (9.42): $\delta E[\boldsymbol{M}] \stackrel{!}{=} 0 \;\overset{\circ}{\Leftrightarrow}$

$$\frac{2\,\mathrm{Re}\left[(\delta \boldsymbol{M}^\dagger)\mathbb{H}_p \boldsymbol{M}\right]}{\boldsymbol{M}^\dagger \mathbb{N}_p \boldsymbol{M}} - \frac{\boldsymbol{M}^\dagger \mathbb{H}_p \boldsymbol{M}}{\left(\boldsymbol{M}^\dagger \mathbb{N}_p \boldsymbol{M}\right)^2} 2\,\mathrm{Re}\left[(\delta \boldsymbol{M}^\dagger)\mathbb{N}_p \boldsymbol{M}\right] \stackrel{!}{=} 0 \tag{9.43}$$

Here we used the standard rules of ↓ *variational calculus*. The real parts show up because $(\delta \boldsymbol{M}^\dagger)\mathbb{H}_p \boldsymbol{M} = [\boldsymbol{M}^\dagger \mathbb{H}_p (\delta \boldsymbol{M})]^*$ since $\mathbb{H}_p$ (and also $\mathbb{N}_p$) are Hermitian (because their expectation values for all vectors $\boldsymbol{M}$ are real).

This must be true For all variations $\delta \boldsymbol{M}^\dagger \rightarrow$

$$\frac{\mathbb{H}_p \boldsymbol{M}}{\boldsymbol{M}^\dagger \mathbb{N}_p \boldsymbol{M}} - \frac{\boldsymbol{M}^\dagger \mathbb{H}_p \boldsymbol{M}}{\left(\boldsymbol{M}^\dagger \mathbb{N}_p \boldsymbol{M}\right)^2} \mathbb{N}_p \boldsymbol{M} \stackrel{!}{=} 0 \tag{9.44}$$

Here we used that all terms in Eq. (9.43) outside of Re[•] are real valued and can be pulled into the real part.

d | Multiply by $\boldsymbol{M}^\dagger \mathbb{N}_p \boldsymbol{M} \rightarrow$

$$\mathbb{H}_p \boldsymbol{M} \stackrel{!}{=} E[\boldsymbol{M}] \cdot \mathbb{N}_p \boldsymbol{M} \tag{9.45}$$

Here we used the definition Eq. (9.42) of $E[\boldsymbol{M}]$.

e | Thus we must solve the ↑ *generalized eigenvalue problem*

$$\mathbb{H}_p \boldsymbol{M} = E \cdot \mathbb{N}_p \boldsymbol{M} \tag{9.46}$$

and search for the eigenvector $\boldsymbol{M}_0$ with lowest eigenvalue $E_0 = E[\boldsymbol{M}]$.

This can be done efficiently with standard linear algebra methods!

→ Replace $M^{[p]}$ by $\boldsymbol{M}_0 \mathrel{\widehat{=}} \tilde{M}^{[p]}$

f | Iterate steps **b** | to **e** | over all sites $p = 1, \ldots, L$

$$|\Psi\rangle = |\{M_i^{[p]}\}\rangle \quad \mapsto \quad |\{\tilde{M}_i^{[p]}\}\rangle = |\tilde{\Psi}\rangle \tag{9.47}$$

This is update of all matrices is called a ⁂ *Sweep*

g | Perform multiple sweeps until $E_{\tilde{\Psi}}$ saturates and $\sigma_H^2(\tilde{\Psi}) \approx 0$

This algorithm is known as

⁂ *(MPS based) Density Matrix Renormalization Group (DMRG)*

- For most systems this algorithm converges remarkably well within a few (5–10) sweeps to the ground state! These simulations are often performed with uniform bond dimension D for all matrices. One typically starts with small bond dimensions $D \sim 10$ and increases D successively to a few hundreds. It is then important to verify that increasing the bond dimension further does not change the outcomes (= expectation values) of the simulation. (Otherwise you known that the simulation drops important Schmidt coefficients!)

- You (implicitly) use this algorithm for numerical simulations on ➔ Problemset 10 to study the → *AKLT model* and the → *Haldane chain*.

11 | Literature:

- The name "density matrix renormalization group" originates from a numerical algorithm that was developed before the invention of matrix product states by WHITE in 1992 [229, 230]. (At the time, it was somehow mysterious why it worked so well.) Only later it was realized that the algorithm could be rephrased in the language of matrix product states and then corresponds to the procedure sketched above [231].
- For a compact, pedagogic introduction to matrix product states, tensor network states, and their applications, see ORÚS [214].
- A more mathematical treatment of matrix product states and their use as variational wave functions to study ground states of many-body Hamiltonians can be found in PEREZ-GARCIA *et al.* [232].
- An extensive (and technical) introduction to matrix product states and their application for DMRG simulations is provided by SCHOLLWÖCK [228]. This is where to start if you want to write your own implementation of DMRG.
- Fortunately, you don't have to do this since there are freely available (and highly optimized) implementations that are easy to use with many programming languages. For `Julia` and `C++`, the library `ITensor` is a good choice [233]. For `Python`, the package `TeNPy` is quite useful [227].

9.3. ‡ Higher dimensions: Tensor network states

It is obvious that the matrix products used to compute MPS wave functions are only a special case of more general index contractions. This immediately suggests a generalization that reflects higher-dimensional geometries …

12 | Generalize MPS topology to higher dimensions (here: 2D):

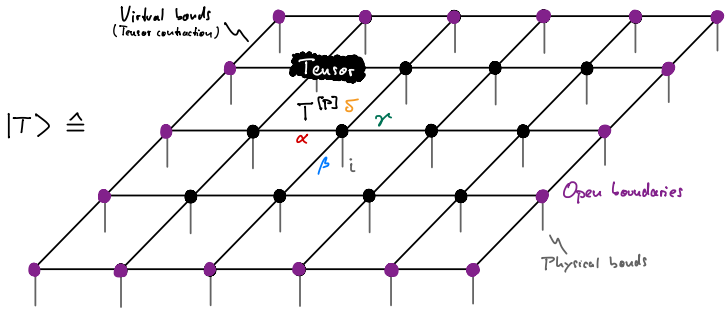

$T^{[p]} \equiv \left(T_i^{[p]}\right)_{\alpha\beta\gamma\delta}$: Tensor of rank (4+1) with …

- physical index $i = 1, \ldots, d$
- virtual indices $\alpha, \beta, \gamma, \delta = 1, \ldots, D$

This defines a ⁂ *Projected entangled pair state (PEPS)* $|T\rangle$ in analogy to Eq. (9.10)

- This generalization was first introduced in Ref. [234].
- Just as for matrix product states in 1D, there are open and periodic boundary PEPS.

- The name "projected entangled pair states" comes from an equivalent interpretation of the local tensors $T^{[p]}$ as linear maps that project from a higher-dimensional auxiliary space into the physical, local Hilbert space (here for 2D),

$$T^{[p]}: \underbrace{\mathbb{C}_p^D \otimes \mathbb{C}_p^D \otimes \mathbb{C}_p^D \otimes \mathbb{C}_p^D}_{\text{Auxiliary Hilbert space on } p} \to \underbrace{\mathbb{C}_p^d}_{\substack{\text{Physical Hilbert} \\ \text{space on } p}}, \tag{9.48}$$

via

$$T^{[p]} = \sum_{i=1}^{d} \sum_{\alpha,\beta,\gamma,\delta=1}^{D} \left(T_i^{[p]}\right)_{\alpha\beta\gamma\delta} |i\rangle_p \langle \alpha, \beta, \gamma, \delta|_p \,. \tag{9.49}$$

It is then easy to see that the PEPS can be constructed by putting a *pair* of auxiliary systems $\mathbb{C}_p^D \otimes \mathbb{C}_{p'}^D$ on each edge $e = (p, p')$ of the lattice, putting them into the fully *entangled state* $|\omega_D\rangle_e = \sum_{n=1}^{D} |n\rangle_p \otimes |n\rangle_{p'}$ (here p and p' are the two adjacent sites connected by the edge e), and then applying the linear map (9.49) onto the product state $|\Omega_D\rangle = \bigotimes_e |\omega_D\rangle_e$ of entangled pairs on all edges:

$$|T\rangle = \left(\prod_p T^{[p]}\right) |\Omega_D\rangle \,. \tag{9.50}$$

I.e., $|T\rangle$ is a state of "projected entangled pairs." Note that this construction also works for MPS, which are therefore 1D versions of PEPS.

13 | While the general formalism of MPS carries over (or generalizes) to PEPS, there is a fundamental difference that prevents an analog of the DMRG algorithm with polynomial scaling in the system size:

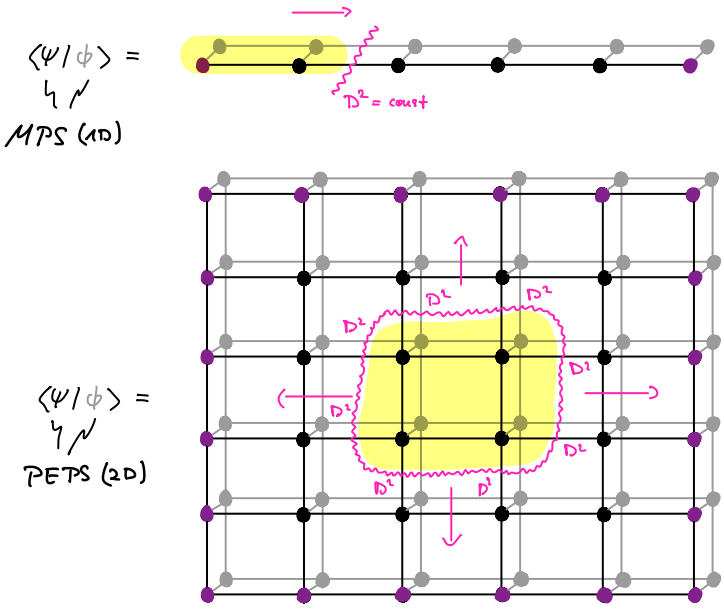

- MPS (1D):

  To compute the overlap of two MPS (or expectation value of a local operator for a given MPS) one can contract the tensor network "along the network" such that the total number of operations scales *polynomially* with the size of the system L (= length of the network).

  → Efficient contractions possible ☺

This efficiency is responsible for the polynomial scaling of the DMRG algorithm sketched in Section 9.2.

- PEPS (2D, 3D, …):

  No matter in which order the contractions of the tensor network are evaluated, one always has to cross a "peak" of $\mathcal{O}(L)$ summations (each over the bond dimension D), so that the number of operations scales like $\mathcal{O}(D^L)$ and therefore *exponentially* in the (linear) system size L.

  → No efficient contractions possible ☹

  One can show rigorously that exact contractions of PEPS are #P-complete [235]. (The complexity class #P is "worse" than the famous complexity class NP!)

→ There is no analog of DMRG for higher dimensions (with similar favorable scaling)

This does not mean that one cannot use tricks (like approximate contractions) to simulate quantum systems in two or higher dimensions. However, the "care-free" situation in 1D – where one can often throw DMRG at the problem without thinking too much – does not carry over to higher dimensions!

14 | Both MPS and PEPS are special families of general ⁂ *Tensor network states (TNS)*:

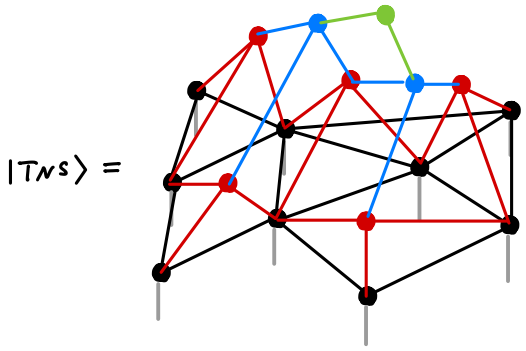

Note that in a generic tensor network state, not every tensor must have physical indices: there can also be "hidden layers" of tensors that connect only trough virtual bonds (colored nodes). This can be useful to mediate long-range entanglement more efficiently. There is of course also no need for a lattice structure.

- General tensor network states (with a focus on MPS and PEPS) are discussed by Orús [214]. A broader (and more recent) overview of different TNS constructions and related numerical algorithms for finding ground states and time-evolution can be found in the review by Orús [236]. A compact, pedagogic overview of TNS constructions and methods can be found in Bañuls [237].
- Tensor network states in 2D (PEPS) are useful tools to (often exactly) describe and characterize quantum states with ← *intrinsic topological order* (like the → *toric code*) [238]. However, there are unexpected subtleties to take into account: local variations of the PEPS tensors do not necessarily correspond to local variations of the Hamiltonian [239] (the PEPS representation of topological order is *unstable*).
- Today, tensor network parametrizations of quantum states are in use in many domains beyond the study of strongly correlated quantum phases. For example, modern TNS-based simulators of *quantum circuits* can often keep up with the available small-scale quantum computers and NISQ devices (NISQ = Noisy intermediate-scale quantum). This is useful to benchmark and validate such devices [240].

10. Symmetry-protected topological phases of interacting spin systems in one-dimension

With the preliminaries in Chapter 8, and the representation of ground states of gapped Hamiltonians by matrix product states discussed in Chapter 9, we are finally equipped to characterize and classify symmetry-protected topological phases of interacting spin systems in 1D. We will again use the bosonic SSH chain to motivate and illustrate general concepts (without rigorously deriving the latter).

The classification of 1D interacting spin systems presented in this chapter was worked out 2011 indepdendently by SCHUCH *et al.* [7] and CHEN *et al.* [6, 29]. Additional insight was by provided by POLLMANN *et al.* for specific classes of systems and symmetries [184, 213, 241].

← *Remember:* (Section 0.5)

> No ← *topological order* in one-dimensional bosonic systems!

→ Symmetries required … (= only SPT phases)

This non-trivial statement can actually be proven by the same MPS-based methods we use in this chapter to classify SPT phases [6, 7].

Rationale:

1. Describe ground states of gapped 1D Hamiltonians by matrix product states.
2. Identify constraints on MPS matrices for symmetric ground states.
3. Use these constraints to characterize/classify SPT phases.

10.1. A working assumption

Before we can execute the procedure sketched above, we should comment on a rather technical problem:

1 | To classify quantum phases, we must come up with a concept that is well-defined in the *Thermodynamic limit*?

◁ Gapped Hamiltonian with PBC on system of length L with unique ground state (GS) $|\Psi\rangle$

→ Problem:

$$\epsilon = \| \underbrace{|\Psi\rangle}_{\text{GS of } H} - \underbrace{|\Psi_D\rangle}_{\text{MPS}} \|^2 \overset{9.36}{\leq} \underbrace{\text{const} \cdot 2^{\text{const} \cdot S_{\max}}}_{\substack{H \text{ gapped} \rightarrow \\ = \text{const (Hastings)}}} \cdot \frac{L}{D^{\text{const}}} \quad \overset{\epsilon \overset{!}{=} \text{const}}{\Longrightarrow} \quad D \xrightarrow{L \to \infty} \infty \tag{10.1}$$

In Section 9.1 we learned that the ground state of gapped, one-dimensional systems can be *approximated* by matrix product states. While the estimate (10.1) is good news for numerical techniques (like DMRG, Section 9.2), it is not enough for a mathematically rigorous classification scheme. First, the error ϵ of approximating an arbitrary gapped ground state by an MPS of low bond dimension is inconvenient as it is unclear how to take it properly into account. A more severe problem is that even when we could take a *constant* error somehow into account, Eq. (10.1) tells us that this can only be achieved with bond dimensions D that diverge with the system size L. But this means that the MPS matrices become "infinitely large" in the thermodynamic limit. This makes it challenging to make rigorous statements in the limit $L \to \infty$.

→ Is there a way out?

2 | Observation:

◁ Ground states of the bosonic SSH chain *at fixpoints*:

$$\text{Phase A:} \quad \underbrace{|A\rangle}_{\text{GS}} \overset{9.22}{=} \underbrace{|\Psi_2\rangle}_{\text{MPS}} \quad \text{with} \quad D = 2 = \text{const} \tag{10.2a}$$

$$\text{Phase B:} \quad \underbrace{|B\rangle}_{\text{GS}} \overset{9.25}{=} \underbrace{|\Psi_0\rangle}_{\text{MPS}} \quad \text{with} \quad D = 0 = \text{const} \tag{10.2b}$$

¡! This is not true for other parameters (= at other points in the same phase).

Experience & Numerical evidence → This is generic …

3 | Working assumption:

In the following, we assume that our findings for the bosonic SSH chain are generally true: Within the equivalence class of one-dimensional, gapped, local, and symmetric Hamiltonians that make up an SPT phase, there are always representatives with *exakt MPS ground states* with *finite bond dimension in the thermodynamic limit*:

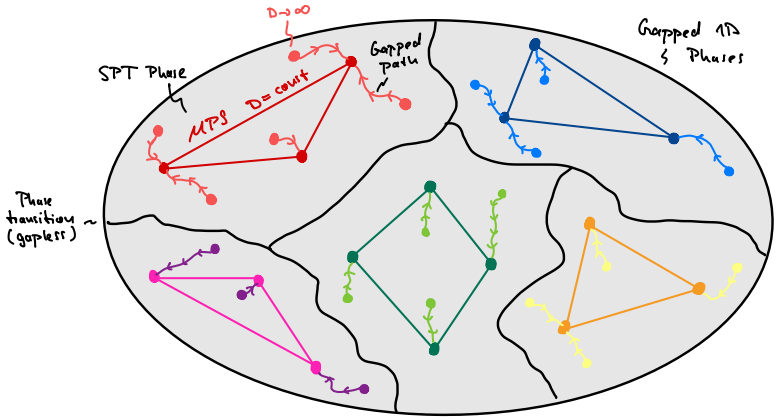

I am not aware of a rigorous proof of this assumption – nor am I aware of any counterexample. CHEN *et al.* write *"We assume that matrix product states capture all possible gapped phases in 1D systems."* [6] Similarly, SCHUCH *et al.* note in their introduction *"[..] ground states of such systems are well approximated by MPS [..], which justifies why we study those phases by considering systems whose ground-state subspace is spanned by MPS [..]."* [7]

→

> Instead of classifying generic ground states, we classify *symmetric matrix product states* with *constant bond dimension*.

10.2. Symmetries of matrix product states

With these preparations, we can now study how (unitary) symmetries – realized as tensor products of local operators – act on the matrices that make up a symmetric matrix product state. This motivates the study of the → *second cohomology group* in Section 10.3 and the concept of → *symmetry fractionalization* and edge modes discussed in Section 10.4. We illustrate these concepts with the fixpoint ground states of the bosonic SSH chain.

4 | ◁ 1D gapped Hamiltonian H with …

- unique ground state $|\Omega\rangle \in \mathcal{H}$
- symmetry group G and *linear* (unitary) representation $\rho : G \to \mathrm{U}(\mathcal{H})$:

$$\forall g \in G : \quad [H, \rho(g)] = 0 \tag{10.3}$$

→ No symmetry breaking:

$$\rho(g)|\Omega\rangle = \alpha(g)|\Omega\rangle \quad \text{with} \quad |\alpha(g)| = 1\,. \tag{10.4}$$

$\alpha : G \to U(1)$: 1D linear representation of G

Question: $|\Omega\rangle$ is MPS →

How does $\rho(g)$ affect the MPS matrices?

5 | Example & Motivation:

◁ Bososnic SSH chain at fixpoint in (topological) phase A:

i | ◁ $x \in D_2$

Let us first check that Eq. (10.4) is satisfied.

→ Action of $\rho(x)$ on $|A\rangle$

$$\rho(x)|A\rangle \overset{8.17}{=} X|A\rangle \overset{8.29}{=} \prod_{k=1}^{L} \sigma^x_{2k}\sigma^x_{2k+1}\,(|0\rangle_{2k}|1\rangle_{2k+1} + |1\rangle_{2k}|0\rangle_{2k+1}) \tag{10.5a}$$

$$\overset{10.4}{\equiv} \alpha(x)|A\rangle \quad ✓ \tag{10.5b}$$

→ $\alpha(x) = 1$

ii | Write $|A\rangle$ as MPS and $\rho(x) = X = \prod_{k=1}^{L} \sigma^x_{2k-1}\sigma^x_{2k} \equiv \prod_{k=1}^{L} \rho_k$

◁ Effect of on-site representation (this is not a symmetry of the Hamiltonian and state!):

$$\rho_k(x)|A\rangle \overset{9.21}{=} \sum_{\dots} \sum_{i_{2k-1},i_{2k}} \mathrm{Tr}\left[\cdots A^{i_{2k-1}i_{2k}} \cdots\right] \sigma^x_{2k-1}\sigma^x_{2k}|\dots i_{2k-1}i_{2k}\dots\rangle \tag{10.6a}$$

$$= \sum_{\dots} \sum_{i,j} \mathrm{Tr}\left[\cdots A^{ij} \cdots\right] \sigma^x_{2k-1}\sigma^x_{2k}|\dots ij\dots\rangle \tag{10.6b}$$

$$\triangleq \sum_{\dots} \sum_{i,j} \mathrm{Tr}\left[\cdots A^{ij} \cdots\right] \sum_{i',j'} (\sigma^x_{2k-1})_{i',i}(\sigma^x_{2k})_{j',j}\,|\dots i'j'\dots\rangle\,. \tag{10.6c}$$

In the second line, we replaced $i_{2k-1} \mapsto i$ and $i_{2k} \mapsto j$ to clean up the notation. In the third line, we expanded the vector $\sigma^x|i\rangle$ into the basis $|i'\rangle$ for $i' \in \{0, 1\}$ using $\sigma^x = \sigma^x_{ij}|i\rangle\langle j|$.

¡! Here we change our notation from A_{ij} to A^{ij} for the physical indices i, j because this allows for a more compact notation → *later*.

iii | Write $(\sigma^x_{2k-1})_{i',i} \equiv \sigma^x_{i'i}$ and $(\sigma^x_{2k})_{j',j} \equiv \sigma^x_{j'j}$ and exchange sums over i, j and i', j'

→

$$\rho_k(x)|A\rangle = \sum_{\cdots} \sum_{i',j'} \mathrm{Tr}\left[\cdots \sum\nolimits_{i,j} \sigma^x_{i'i}\sigma^x_{j'j} A^{ij} \cdots\right] |\ldots i'j' \ldots\rangle \tag{10.7a}$$

$$\equiv \underbrace{\sum_{\cdots} \sum_{i',j'} \mathrm{Tr}\left[\cdots \tilde{A}^{i'j'} \cdots\right] |\ldots i'j' \ldots\rangle}_{\text{New MPS}} \tag{10.7b}$$

with Transformed matrix

$$\underbrace{\tilde{A}^{i'j'}}_{\substack{2\times 2\text{-matrices} \\ (\text{for every } i'j')}} = \sum_{i,j} \sigma^x_{i'i}\sigma^x_{j'j} A^{ij} \tag{10.8}$$

That is, $\rho_k(x)|A\rangle$ is a new MPS (with the same bond dimension) where the matrix A on site k is replaced by the new matrix $\tilde{A}$.

¡! So far, this result does not depend on the specific form of the matrices A. In particular, it does not depend on the invariance Eq. (10.5) of the MPS under the symmetry.

iv | We can evaluate Eq. (10.8) explicitly for our case:

$$\tilde{A}^{i'j'}_{\alpha\beta} \overset{10.8}{=} \sum_{i,j} \sigma^x_{i'i}\sigma^x_{j'j} A^{ij}_{\alpha\beta} \tag{10.9a}$$

$$\overset{9.23}{=} \sum_{i} \sigma^x_{i'i}\delta_{i\alpha} \sum_{j} \sigma^x_{j'j}\sigma^x_{j\beta} \tag{10.9b}$$

$$\overset{\circ}{=} \sum_{\alpha'} \sigma^x_{\alpha'\alpha}\,\delta_{i'\alpha'} \sum_{\beta'} \sigma^x_{j'\beta'}\,\sigma^x_{\beta'\beta} \tag{10.9c}$$

$$= \sum_{\alpha',\beta'} \sigma^x_{\alpha'\alpha} \left(\delta_{i'\alpha'}\,\sigma^x_{j'\beta'}\right) \sigma^x_{\beta'\beta} \tag{10.9d}$$

$$\overset{9.23}{=} \alpha_k(x) \left[\hat{\sigma}^{x\dagger} \cdot A^{i'j'} \cdot \hat{\sigma}^x\right]_{\alpha\beta} \tag{10.9e}$$

Here we reorganized the sums in the third and fourth line and introduced $\alpha_k(x) = 1$ in the last line.

- ¡! In the last line, we write the Pauli matrices with a hat $\hat{\bullet}$ to emphasize that they act on the *virtual* indices α and β, whereas the original Pauli matrices of the representation $\rho(x)$ act on the *physical* indices i and j.
- ¡! That this translation of the symmetry acting on physical indices to virtual indices works is *not* generic but a feature of the matrices A (more generally: the symmetry of the MPS, see → *below*).

v | We can now re-express the invariance Eq. (10.5) of $|A\rangle$ in the language of MPS:

◁ *Global* symmetry $\rho(x) = \prod_{k=1}^{L} \rho_k$:

$$\rho(x)|A\rangle \overset{10.7}{=} \sum_{\boldsymbol{i}} \mathrm{Tr}\left[\tilde{A}^{i_1 i_2} \tilde{A}^{i_3 i_4} \cdots \tilde{A}^{i_{2L-1} i_{2L}}\right] |i_1 i_2, \ldots, i_{2L-1} i_{2L}\rangle \tag{10.10a}$$

$$\overset{10.9}{=} \alpha(x) \sum_{\boldsymbol{i}} \mathrm{Tr}\left[\hat{\sigma}^{x\dagger} A^{i_1 i_2} \hat{\sigma}^{x} \hat{\sigma}^{x\dagger} A^{i_3 i_4} \hat{\sigma}^{x} \cdots \hat{\sigma}^{x\dagger} A^{i_{2L-1} i_{2L}} \hat{\sigma}^{x}\right] \times |i_1 i_2, \ldots, i_{2L-1} i_{2L}\rangle \tag{10.10b}$$

$$= \alpha(x) \sum_{\boldsymbol{i}} \mathrm{Tr}\left[A^{i_1 i_2} A^{i_3 i_4} \cdots A^{i_{2L-1} i_{2L}}\right] |i_1 i_2, \ldots, i_{2L-1} i_{2L}\rangle \tag{10.10c}$$

$$= \alpha(x)|A\rangle\,, \tag{10.10d}$$

Here we used the cyclicity of the trace and defined $\alpha(x) \equiv \prod_k \alpha_k(x)$.

vi | ◁ $z \in D_2$:

Along the same lines one can show for the transformation under $\rho_k(z)$ the following:

$$\tilde{A}^{i'j'} \doteq \alpha_k(z)\, \hat{\sigma}^{z\dagger} A^{i'j'} \hat{\sigma}^{z} \quad \text{with} \quad \alpha_k(z) = -1 \tag{10.11}$$

such that

$$\rho(z)|A\rangle = \alpha(z)|A\rangle \quad \text{with} \quad \alpha(z) = (-1)^L \tag{10.12}$$

This is again consistent with Eq. (10.4).

6 | These results (shown here for a specific example) are valid in general:

◁ Linear unitary representation of G of the form

$$\rho(g) = \pi(g) \otimes \pi(g) \cdots \otimes \pi(g) \tag{10.13}$$

$\pi : G \to \mathbb{C}^{d\times d}$: Linear unitary on-site representation

In our example above, it was $\pi(g) = \rho_k(g)$ with $d = 4 = 2 \cdot 2$ (since we combined two spin-$\frac{1}{2}$ into one physical site), recall Eq. (8.13).

◁ MPS $|M\rangle$ invariant under $\rho(g)$ (up to a phase):

$$\rho(g)|M\rangle = \alpha(g)|M\rangle \tag{10.14}$$

Here we restrict ourselves to translation invariant MPS of the form (9.29) to make our lives easier. Conceptually this is not necessary for what follows!

$\overset{*}{\to}$ (↑ Refs. [29, 242])

$$\boxed{\sum_j [\pi(g)]_{ij} M^j = \gamma(g)\, V^\dagger(g) \cdot M^i \cdot V(g)} \tag{10.15}$$

Here "$\cdot$" denote $D \times D$-matrix products.

$\gamma(g) \in \mathrm{U}(1)$: 1D linear unitary representation of G

$V(g) \in \mathbb{C}^{D\times D}$: Invertible (unitary) $D \times D$-matrices

- Eq. (10.15) is valid under certain technical assumptions; see Ref. [243, Chapters III and IV] for more details. For the MPS we are interested in (= unique ground states of gapped Hamiltonians), these conditions are met and we can assume Eq. (10.15) to hold for all states of interest.
- For MPS that are *not translation invariant*, the left- and right unitary matrices $V^\dagger(g)$ and $V(g)$ can be different (i.e., not adjoint) as they must cancel with the corresponding matrices from their neighboring sites (which can be different).